

Hydrothermal synthesis, crystal structure, and characterization of a new pseudo-two-dimensional uranyl oxyfluoride, $[\text{N}(\text{C}_2\text{H}_5)_4]_2[(\text{UO}_2)_4(\text{OH}_2)_3\text{F}_{10}]$

Kang Min Ok, Dermot O'Hare*

Chemistry Research Laboratory, University of Oxford, Oxford, OX1 3TA, UK

Received 12 October 2006; received in revised form 31 October 2006; accepted 1 November 2006

Available online 10 November 2006

Abstract

A new uranyl oxyfluoride, $[\text{N}(\text{C}_2\text{H}_5)_4]_2[(\text{UO}_2)_4(\text{OH}_2)_3\text{F}_{10}]$ has been synthesized by a hydrothermal reaction technique using $(\text{C}_2\text{H}_5)_4\text{NBr}$, $\text{UO}_2(\text{OCOCH}_3)_2 \cdot 2\text{H}_2\text{O}$, and HF as reagents. The structure of $[\text{N}(\text{C}_2\text{H}_5)_4]_2[(\text{UO}_2)_4(\text{OH}_2)_3\text{F}_{10}]$ has been determined by a single-crystal X-ray diffraction technique. $[\text{N}(\text{C}_2\text{H}_5)_4]_2[(\text{UO}_2)_4(\text{OH}_2)_3\text{F}_{10}]$ crystallizes in the monoclinic space group $P2_1/n$ (No. 14), with $a = 13.852(3) \text{ \AA}$, $b = 15.532(3) \text{ \AA}$, $c = 16.481(3) \text{ \AA}$, $\beta = 98.88(3)^\circ$, $V = 3503.4(12) \text{ \AA}^3$, and $Z = 4$. $[\text{N}(\text{C}_2\text{H}_5)_4]_2[(\text{UO}_2)_4(\text{OH}_2)_3\text{F}_{10}]$ reveals a novel pseudo-two-dimensional crystal structure that is composed of UO_2F_5 , UO_3F_4 , and UO_4F_3 pentagonal bipyramids. Each uranyl pentagonal bipyramid shares edges and corners through F atoms to form a six-membered ring. The rings are further interconnected to generate infinite strips running along the b -axis. $[\text{N}(\text{C}_2\text{H}_5)_4]_2[(\text{UO}_2)_4(\text{OH}_2)_3\text{F}_{10}]$ has been further characterized by elemental analysis, bond valence calculations, Infrared and Raman spectroscopy, and thermogravimetric analysis.

© 2006 Elsevier Inc. All rights reserved.

Keywords: Synthesis; Uranyl oxyfluoride; Pseudo-two-dimensional structure

1. Introduction

The hydrothermal synthesis of new materials has been studied extensively and is well-established [1–8]. This approach is an effective method of increasing the solubility and the reactivity of the reagents, by using the acid or base mineralizers in the synthesis [9,10]. The choice of appropriate organic or inorganic structure-directing agents is an important factor that significantly affects the outcome of these reactions [1,2,11]. Although the exact function of the structure-directing agents on the assembly and subsequent crystallization of the extended structures is still rudimentarily understood, templating agents are now routinely used in hydrothermal syntheses. The main reason for this routine use of templates might be due to some observed correlation between the framework structures of the materials and the templates employed, which includes charge-balancing, size, and pH effects of the structure-

directing agents. Most of the cations in the periodic table have been used in hydrothermal reactions as framework materials. Among many cations, the actinides elements can allow access to structurally versatile materials due to the great spatial extend of the $5f$ orbitals and higher coordination numbers. We have extensively explored hydrothermal synthesis of uranium (VI) compounds containing the uranyl group [12–22], since uranyl materials not only suggest structural variability but also promise potential applications such as catalyst, ion-exchange, intercalation, and fast ion conductors [23–27]. With these ideas in mind, we have used a hydrothermal reaction technique to synthesize a new organically templated uranium oxide fluoride. Many uranium oxide fluoride materials have been reported to date [13,28–40]. Although variable structural dimensions have been observed, most uranyl materials adapt layered structures [41–45]. We have reported an organically templated microporous uranium oxide fluoride by using $[\text{C}_4\text{N}_2\text{H}_{12}]^{2+}$ and $[\text{N}(\text{CH}_3)_4]^+$ cations as templating cations [13,46]. In this paper, we introduce the $[\text{N}(\text{C}_2\text{H}_5)_4]^+$ cation and report the hydrothermal

*Corresponding author. Fax: +44 1865 285131.

E-mail address: dermot.ohare@chem.ox.ac.uk (D. O'Hare).

synthesis, crystal structure, and characterizations of $[\text{N}(\text{C}_2\text{H}_5)_4]_2[(\text{UO}_2)_4(\text{OH}_2)_3\text{F}_{10}]$, representing a new pseudo-two-dimensional uranium oxide fluoride material with a novel structure containing hydrogen bonds.

2. Experimental

2.1. Synthesis

Caution! Although all uranium materials used in these experiments were depleted, extra care and good laboratory practice should always be used when handling uranium containing materials. HF is toxic and corrosive.

$(\text{C}_2\text{H}_5)_4\text{NBr}$ (Aldrich, 99%) and HF (BDH, 40%) were used as received. $\text{UO}_2(\text{CH}_2\text{CO}_2)_2 \cdot 2\text{H}_2\text{O}$ was prepared from UO_3 (99.8%, Strem) [47]. Single-crystals of $[\text{N}(\text{C}_2\text{H}_5)_4]_2[(\text{UO}_2)_4(\text{OH}_2)_3\text{F}_{10}]$ were prepared by using 0.425 g (1.00 mmol) of $\text{UO}_2(\text{CH}_2\text{CO}_2)_2 \cdot 2\text{H}_2\text{O}$, 0.210 g (1.00 mmol) of $(\text{C}_2\text{H}_5)_4\text{NBr}$, 0.18 mL of HF (aq. 40%), and 2 mL of deionized water. All reactants were transferred in a Teflon lined 23 ml stainless steel autoclave. The autoclave was heated to 180 °C at 1 °C min⁻¹, where the temperature was held constant for 72 h. The reaction was cooled to room temperature at 6 °C h⁻¹, and the autoclave opened. Yellow single-crystals were recovered using filtration, and washed with water and acetone, and allowed to

dry in air. A yield of 41% based on uranium was observed. Powder X-ray diffraction (XRD) on the ground crystals indicated a single-phase product, and was in a good agreement with the calculated pattern from the single-crystal structure (see supporting information).

2.2. Crystallographic determination

The structure of $[\text{N}(\text{C}_2\text{H}_5)_4]_2[(\text{UO}_2)_4(\text{OH}_2)_3\text{F}_{10}]$ was determined by standard crystallographic methods. A yellow block crystal (0.04 × 0.12 × 0.18 mm³) was used for single-crystal XRD. The data were collected using an Enraf Nonius FR 590 Kappa CCD diffractometer with graphite monochromated $\text{MoK}\alpha$ radiation. The crystal was mounted on a glass fiber using *N*-paratone oil and cooled in situ using an Oxford Cryostream 600 Series to 150 K for data collection. Frames were collected, indexed, and processed using Denzo SMN and the files scaled together using HKL GUI within Denzo SMN [48]. The heavy atom positions were determined using SIR97 [49]. All other sites were located from Fourier difference maps. All atoms were refined using anisotropic thermal parameters using full matrix least squares procedures. All calculations were performed using the WinGX 98 crystallographic software package [50]. The final Fourier difference map revealed minimum and maximum peaks of 2.168 and $-1.501 \text{ e}\text{\AA}^{-3}$.

Table 1
Crystal data for $[\text{N}(\text{C}_2\text{H}_5)_4]_2[(\text{UO}_2)_4(\text{OH}_2)_3\text{F}_{10}]$

Empirical formula	$[\text{N}(\text{C}_2\text{H}_5)_4]_2[(\text{UO}_2)_4(\text{OH}_2)_3\text{F}_{10}]$
Formula weight	1584.64
Crystal system	Monoclinic
Space group	$P2_1/n$ (No. 14)
Z	4
a (Å)	13.852(3)
b (Å)	15.532(3)
c (Å)	16.482(3)
β (°)	98.88(3)
Volume (Å ³)	3503.6(12)
Temperature (K)	150.0(2)
ρ_{calc} (g cm ⁻³)	3.004
μ (mm ⁻¹)	1.853
Crystal color	Yellow
Crystal habit	Block
Crystal size	0.04 × 0.12 × 0.18
Reflections collected	15548
Independent reflections	7959
R(int)	0.0410
$T_{\text{min}}, T_{\text{max}}$	0.08, 0.47
No. of parameters	429
Goodness-of-fit on F^2	1.088
X-ray radiation (λ , Å)	$\text{MoK}\alpha$ (0.71073)
θ Range (°)	5.14–27.50
Limiting indices	$-17 \leq h \leq 17, -20 \leq k \leq 20, -21 \leq l \leq 21$
Refinement method	Full-matrix least-squares on F^2 [SHELXL-97]
Final $R^{\text{a,b}}$ indices [$I > 3\sigma(I)$]	$R(F) = 0.0376, R_w(F_o^2) = 0.0728$
R indices (all data)	$R(F) = 0.0631, R_w(F_o^2) = 0.0787$
Largest diff. peak and hole ($\text{e}\text{\AA}^{-3}$)	2.168 and -1.501

^a $R(F) = \sum ||F_o| - |F_c|| / \sum |F_o|$.

^b $R_w(F_o^2) = [\sum w(F_o^2 - F_c^2)^2 / \sum w(F_o^2)]^{1/2}$.

Crystallographic data, atomic coordinates and displacement parameters, and selected bond distances for $[\text{N}(\text{C}_2\text{H}_5)_4]_2[(\text{UO}_2)_4(\text{OH}_2)_3\text{F}_{10}]$ are given in Tables 1–3. The X-ray powder diffraction data were collected on a PANalytical X'Pert Pro diffractometer using $\text{CuK}\alpha$ radiation at room temperature with 40 kV and 40 mA in the 2θ range 5–60° with a step size of 0.02°, and a step time of 1 s.

2.3. Elemental analysis

C, H, and N analyses were conducted using an Elementar Vario EL analyzer. The composition of the U was determined by inductively coupled plasma (ICP) analysis using a Thermo Jarrell Ash Scan 16 instrument.

Elemental microanalysis for $[\text{N}(\text{C}_2\text{H}_5)_4]_2[(\text{UO}_2)_4(\text{OH}_2)_3\text{F}_{10}]$ obsd (calcd): U, 59.88% (60.08%); N, 1.75% (1.77%); C, 11.93% (12.13%); H, 2.78% (2.93%).

2.4. Spectroscopic characterizations

Infrared spectra were recorded on a Bio-Rad FTS 6000 FT-IR spectrometer in the 400–4000 cm^{-1} range, with the sample intimately contacted by a diamond as an attenuated total reflectance (ATR) crystal. Raman spectra were recorded at room temperature on a Jobin Yvon spectrometer (Labram 1B) equipped with a microscope, through a 50-fold magnification objective (Olympus Company). A 40 mW Argon-ion Laser (514 nm) was used.

Table 2
Atomic coordinates for $[\text{N}(\text{C}_2\text{H}_5)_4]_2[(\text{UO}_2)_4(\text{OH}_2)_3\text{F}_{10}]$

Atom	x	y	z	U_{eq}^a (\AA^2)
U(1)	0.4814(1)	0.1150(1)	0.2396(1)	0.016(1)
U(2)	0.5910(1)	0.3903(1)	0.2680(1)	0.017(1)
U(3)	0.6261(1)	−0.1478(1)	0.2241(1)	0.018(1)
U(4)	0.4549(1)	0.6564(1)	0.2381(1)	0.017(1)
F(1)	0.3385(4)	0.0496(3)	0.2170(4)	0.033(1)
F(2)	0.5456(3)	0.2487(3)	0.2715(4)	0.033(2)
F(3)	0.5418(4)	−0.0208(3)	0.2177(4)	0.028(1)
F(4)	0.4267(3)	0.3872(3)	0.2687(4)	0.026(1)
F(5)	0.5487(4)	0.5333(3)	0.2635(4)	0.030(1)
F(6)	0.7214(3)	0.2927(3)	0.2677(4)	0.035(2)
F(7)	0.7539(3)	−0.0429(3)	0.2272(4)	0.029(1)
F(8)	0.4683(3)	−0.1947(3)	0.2175(4)	0.026(1)
F(9)	0.6145(3)	−0.2970(3)	0.2334(4)	0.027(1)
F(10)	0.3072(4)	0.7077(3)	0.2241(5)	0.047(2)
O(1)	0.4869(4)	0.0945(4)	0.3448(4)	0.027(2)
O(2)	0.4794(5)	0.1364(4)	0.1347(4)	0.027(1)
O(3)	0.5737(4)	0.3903(4)	0.1608(4)	0.028(2)
O(4)	0.6095(5)	0.3915(4)	0.3758(4)	0.031(2)
O(5)	0.6402(4)	−0.1431(4)	0.3312(4)	0.025(1)
O(6)	0.6134(5)	−0.1524(4)	0.1166(4)	0.031(2)
O(7)	0.4707(5)	0.6730(4)	0.3444(4)	0.032(2)
O(8)	0.4400(5)	0.6373(4)	0.1318(4)	0.037(2)
OW(1)	0.3585(4)	0.2267(4)	0.2401(4)	0.028(2)
OW(2)	0.6677(4)	0.1153(4)	0.2585(4)	0.028(2)
OW(3)	0.3402(4)	0.5358(4)	0.2468(4)	0.024(1)
N(1)	0.7654(5)	0.1287(4)	0.9857(5)	0.021(2)
N(2)	0.2626(6)	0.8872(5)	0.4683(5)	0.029(2)
C(11)	0.7406(7)	0.1764(6)	1.0609(6)	0.030(2)
C(111)	0.6628(9)	0.2420(7)	1.0452(8)	0.046(3)
C(12)	0.8350(7)	0.0572(6)	1.0180(6)	0.028(2)
C(121)	0.8710(8)	0.0029(6)	0.9517(7)	0.036(3)
C(13)	0.6732(7)	0.0924(6)	0.9369(6)	0.029(2)
C(131)	0.6158(8)	0.0337(7)	0.9812(8)	0.044(3)
C(14)	0.8114(7)	0.1885(6)	0.9290(6)	0.029(2)
C(141)	0.9087(8)	0.2272(7)	0.9656(8)	0.040(3)
C(21)	0.3054(7)	0.8875(6)	0.3896(7)	0.032(2)
C(211)	0.4149(8)	0.8853(7)	0.4011(8)	0.043(3)
C(22)	0.2907(8)	0.8034(7)	0.5168(7)	0.037(3)
C(221)	0.2589(10)	0.7221(7)	0.4710(8)	0.051(3)
C(23)	0.1522(7)	0.8924(7)	0.4434(7)	0.038(3)
C(231)	0.0927(9)	0.8891(13)	0.5142(10)	0.078(5)
C(24)	0.2998(8)	0.9599(7)	0.5224(6)	0.038(3)
C(241)	0.2857(12)	1.0479(7)	0.4831(8)	0.064(4)

^a U_{eq} is defined as one third of the trace of the orthogonalized U_{ij} tensor.

Table 3
Selected bond distances (Å) and bond valence calculations for $[\text{N}(\text{C}_2\text{H}_5)_4]_2[(\text{UO}_2)_4(\text{OH}_2)_3\text{F}_{10}]$

Bond distances		Bond valence	Bond distances	
U(1)–O(1)	1.754(7)	1.772	N(1)–C(11)	1.527(12)
U(1)–O(2)	1.755(6)	1.769	N(1)–C(12)	1.514(11)
U(1)–F(1)	2.206(5)	0.568	N(1)–C(13)	1.510(11)
U(1)–F(2)	2.287(4)	0.464	N(1)–C(14)	1.525(12)
U(1)–F(3)	2.318(4)	0.430		
U(1)–OW(1)	2.432(6)	0.480	N(2)–C(21)	1.508(13)
U(1)–OW(2)	2.550(6)	0.382	N(2)–C(22)	1.546(12)
Bond valence sum of U(1)		5.865	N(2)–C(23)	1.522(13)
			N(2)–C(24)	1.481(13)
U(2)–O(3)	1.746(7)	1.800		
U(2)–O(4)	1.755(7)	1.769	C(11)–C(111)	1.476(14)
U(2)–F(2)	2.290(4)	0.461	C(12)–C(121)	1.524(14)
U(2)–F(4)	2.279(5)	0.474	C(13)–C(131)	1.476(15)
U(2)–F(5)	2.296(5)	0.454	C(14)–C(141)	1.514(14)
U(2)–F(6)	2.358(5)	0.389		
U(2)–F(7)	2.376(5)	0.372	C(21)–C(211)	1.499(15)
Bond valence sum of U(2)		5.719	C(22)–C(221)	1.503(16)
			C(23)–C(231)	1.529(18)
U(3)–O(5)	1.747(6)	1.796	C(24)–C(241)	1.514(17)
U(3)–O(6)	1.754(7)	1.772		
U(3)–F(3)	2.286(4)	0.465		
U(3)–F(6)	2.291(5)	0.460		
U(3)–F(7)	2.400(5)	0.350		
U(3)–F(8)	2.292(5)	0.458		
U(3)–F(9)	2.330(4)	0.417		
Bond valence sum of U(3)		5.718		
U(4)–O(7)	1.752(7)	1.779		
U(4)–O(8)	1.757(7)	1.762		
U(4)–F(5)	2.313(5)	0.435		
U(4)–F(8)	2.349(4)	0.398		
U(4)–F(9)	2.339(5)	0.408		
U(4)–F(10)	2.176(5)	0.613		
U(4)–OW(3)	2.474(5)	0.443		
Bond valence sum of U(4)		5.838		

The 1800 L/mm grating provides a resolution starting from 1.5 cm^{-1} at 200 cm^{-1} up to 1.0 cm^{-1} at 3600 cm^{-1} . The abscissa was calibrated with the 520.7 cm^{-1} peak of a silicon standard, and the sharp Raman shifts are accurate within the limits of the resolution.

2.5. Thermogravimetric analysis

Thermogravimetric analysis was performed on a STA 409 PC Thermogravimetric Analyzer (NETZSCH Instruments). The polycrystalline $[\text{N}(\text{C}_2\text{H}_5)_4]_2[(\text{UO}_2)_4(\text{OH}_2)_3\text{F}_{10}]$ sample was contained within an alumina crucible and heated at a rate of $10\text{ }^\circ\text{C min}^{-1}$ from room temperature to $800\text{ }^\circ\text{C}$ under flowing nitrogen.

3. Results and discussion

3.1. Structure

$[\text{N}(\text{C}_2\text{H}_5)_4]_2[(\text{UO}_2)_4(\text{OH}_2)_3\text{F}_{10}]$ is a new pseudo-two-dimensional uranyl oxyfluoride compound containing chains that run parallel to the *b*-axis (see Fig. 1). The

chains are composed of UO_2F_5 , UO_3F_4 , and UO_4F_3 pentagonal bipyramids connected by U–F–U bonds. As can be seen in Fig. 2, the two $[\text{U}(2)\text{O}_2\text{F}_5]$ and $[\text{U}(3)\text{O}_2\text{F}_5]$ pentagonal bipyramids share edges through F(6) and F(7) and form $\text{U}_2\text{O}_4\text{F}_8$ dimers. These $\text{U}_2\text{O}_4\text{F}_8$ dimers are further connected by the $[\text{U}(1)\text{O}_2\text{F}_3(\text{OH}_2)_2]$ group through F(2) and F(3) as well as to the $[\text{U}(4)\text{O}_2\text{F}_4(\text{OH}_2)]$ group through F(5), F(8), and F(9). From these connections of pentagonal bipyramids, a novel six-membered ring can be formed (see Figs. 1 and 2). Intra-chain connection is further made from each six-membered ring through F(3) and F(5) so that infinite bands are observed along [010] direction (see Fig. 3). There are four crystallographically unique U^{6+} cations in the $[\text{N}(\text{C}_2\text{H}_5)_4]_2[(\text{UO}_2)_4(\text{OH}_2)_3\text{F}_{10}]$ structure. All U^{6+} cations are in pentagonal bipyramids environments connected to oxygen or fluorine atoms. The short uranyl U=O bond distances for each U^{6+} cation range from 1.746(7) to 1.757(7) Å. The U–F distances are ranging from 2.176(5) to 2.400(5) Å. The equatorial U–OH₂ distances for U(1) and U(4) range from 2.432(6) to 2.550(6) Å. The observed longer U–O distances are owing to the hydrogen bonds of coordinated water molecules. The assignment of

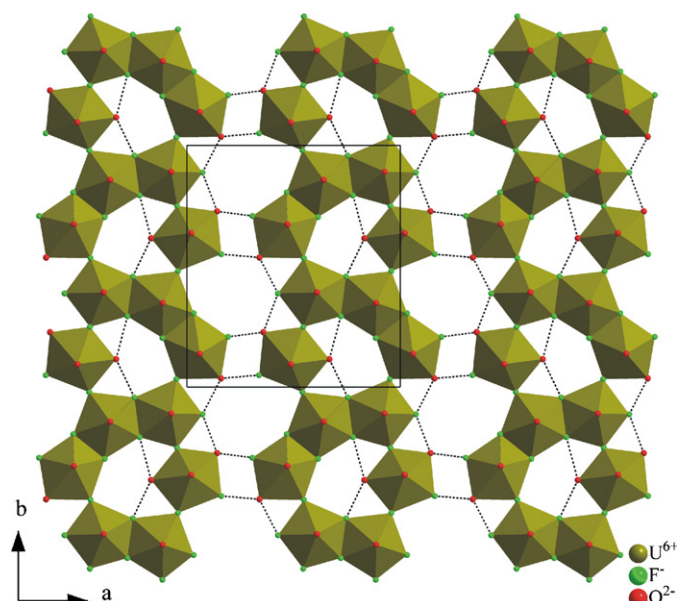


Fig. 1. Polyhedral representation of $[\text{N}(\text{C}_2\text{H}_5)_4]_2[(\text{UO}_2)_4(\text{OH}_2)_3\text{F}_{10}]$ in the ab -plane. The dashed lines indicate O–F hydrogen bonding, giving the structure a pseudo-two-dimensional topology. Note the novel six-membered rings and chains running along the b -axis. Tetraethylammonium cations have been removed for clarity.

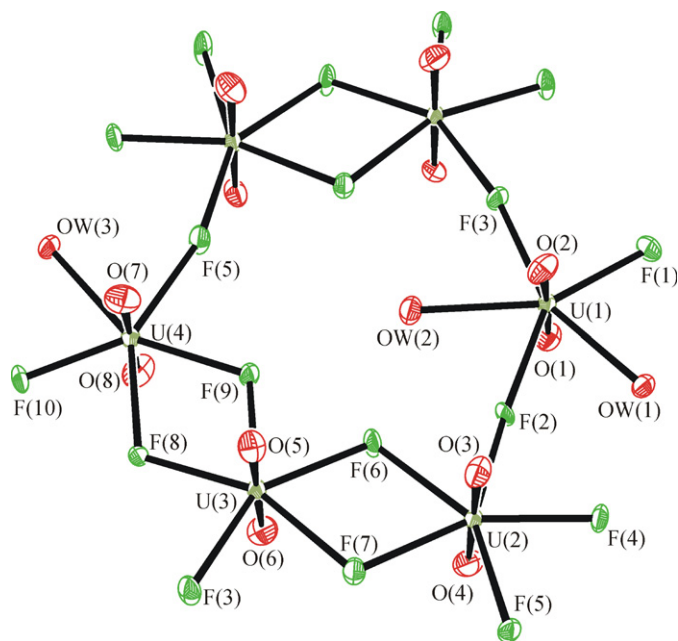


Fig. 2. ORTEP (50% probability ellipsoids) drawing of $[\text{N}(\text{C}_2\text{H}_5)_4]_2[(\text{UO}_2)_4(\text{OH}_2)_3\text{F}_{10}]$ in the ab -plane. Tetraethylammonium cations have been removed for clarity. Note the pentagonal bipyramidal environments of U^{6+} cations to form a novel six-membered ring.

fluoride anions and bound water molecules was based upon bond length and hydrogen-bonding interactions, which is consistent with values of previously reported [20]. Besides, subsequent refinement with oxygen atoms for the fluorine positions not only results in slightly worse final R values but also reveals nonpositive definite on the displacement parameters, which clearly confirms our model. In order to

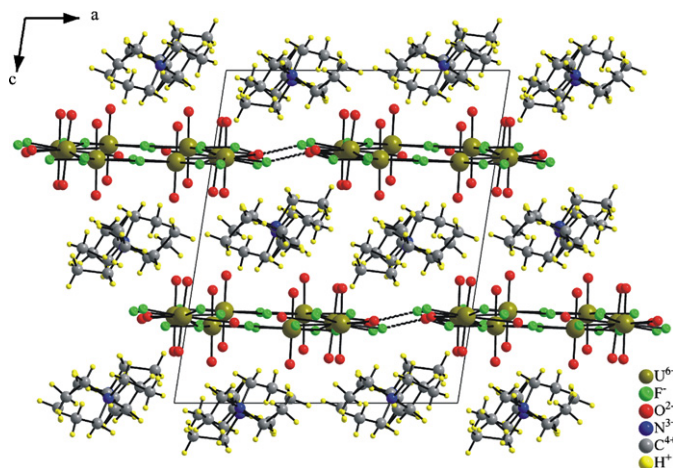


Fig. 3. Ball-and-stick diagram of $[\text{N}(\text{C}_2\text{H}_5)_4]_2[(\text{UO}_2)_4(\text{OH}_2)_3\text{F}_{10}]$ in the ac -plane. Note the inter-chain hydrogen bonds between coordinated water and F atoms, which generate a pseudo-two-dimensional topology in $[\text{N}(\text{C}_2\text{H}_5)_4]_2[(\text{UO}_2)_4(\text{OH}_2)_3\text{F}_{10}]$. Bulky tetraethylammonium cations reside in between anionic pseudo-layers in order to maintain charge neutrality.

identify the positions of H^+ , the hydrogen bonds in the structure were analyzed. We observe that strong inter- and intra-chain hydrogen bonds occur from coordinated water molecules, OW(1), OW(2), and OW(3) to the adjacent fluorine atoms [OW(1)⋯F(10) 2.474(16) Å; OW(1)⋯F(4) 2.681(5) Å; OW(2)⋯F(6) 2.85(10) Å; OW(2)⋯F(7) 2.815(7) Å; OW(3)⋯F(1) 2.642(17) Å; OW(3)⋯F(4) 2.600(5) Å] (see dashed lines drawn in Fig. 1). The inter-chain hydrogen bonds might give $[\text{N}(\text{C}_2\text{H}_5)_4]_2[(\text{UO}_2)_4(\text{OH}_2)_3\text{F}_{10}]$ a pseudo-two-dimensional topology. Bond valence calculations on these water molecules and terminal fluorine atom sites also reveal relatively smaller values (see Table 3), which are consistent with our model. Finally, the IR spectrum confirms the presence of coordinated OH_2 group (see spectroscopic studies). In connectivity terms, $[\text{N}(\text{C}_2\text{H}_5)_4]_2[(\text{UO}_2)_4(\text{OH}_2)_3\text{F}_{10}]$ can be formulated as consisting of $\{[\text{U}(1)\text{O}_{2/1}(\text{OH}_2)_2\text{F}_{2/2}\text{F}_{1/1}]^0 [\text{U}(2)\text{O}_{2/1}\text{F}_{4/2}\text{F}_{1/1}]^- [\text{U}(3)\text{O}_{2/1}\text{F}_{5/2}]^{0.5-} [\text{U}(4)\text{O}_{2/1}(\text{OH}_2)\text{F}_{3/2}\text{F}_{1/1}]^{0.5-}\}^{2-}$ anionic chains, with charge balance maintained by the two bulky $[\text{N}(\text{C}_2\text{H}_5)_4]^+$ organic cations. Bond valence calculations [51–53] resulted in values range from 5.72 to 5.87 for U^{6+} cations. With relatively smaller organic template, $[\text{N}(\text{CH}_3)_4]^+$ cation, in the similar synthesis condition, a three-dimensional open-framework uranium oxide fluoride, $[\text{N}(\text{CH}_3)_4]_2[(\text{UO}_2)_2\text{F}_3]$ (MUF-2) has been obtained [46]. MUF-2 contains ten-membered ring (10-MR) channels running along the [100] and [010] directions. However, using the relatively bigger organic template, $[\text{N}(\text{C}_2\text{H}_5)_4]^+$ cation, produces a novel pseudo-two-dimensional oxide fluoride, $[\text{N}(\text{C}_2\text{H}_5)_4]_2[(\text{UO}_2)_4(\text{OH}_2)_3\text{F}_{10}]$. This is perhaps because of the nature of the uranyl moiety to adapt a two-dimensional layered structure easily owing to its pentagonal pyramidal geometry. Besides, the tetraethyl ammonium cation comparing to the tetramethyl ammonium cation, is too big to be included in any channel structure.

3.2. Infrared and Raman spectroscopy

The infrared and Raman spectra of $[\text{N}(\text{C}_2\text{H}_5)_4]_2[(\text{UO}_2)_4(\text{OH}_2)_3\text{F}_{10}]$ revealed $\text{U}=\text{O}$ and $\text{U}-\text{F}$ stretches at ca. $840\text{--}920\text{ cm}^{-1}$ and at ca. $190\text{--}470\text{ cm}^{-1}$, respectively. The CH_2 and CH_3 vibrations of tetraethylammonium group are observed in both the IR and Raman and found around $1390\text{--}1460$ and $2930\text{--}3020\text{ cm}^{-1}$. Vibrations attributable to the coordinated H_2O were observed at ca. 1660 and 3500 cm^{-1} . The IR and Raman vibrations and assignments are listed in Table 4. The assignments are consistent with those previously reported [54,55].

3.3. Thermogravimetric analysis

The thermal behavior of $[\text{N}(\text{C}_2\text{H}_5)_4]_2[(\text{UO}_2)_4(\text{OH}_2)_3\text{F}_{10}]$ was investigated using thermogravimetric analysis. $[\text{N}(\text{C}_2\text{H}_5)_4]_2[(\text{UO}_2)_4(\text{OH}_2)_3\text{F}_{10}]$ shows a weight loss of 3.45% between 140 and 160°C that is attributed to the loss of the coordinated water molecules from the material (Calcd 3.41%). Tetramethylammonium group and one mole of F_2 are lost at around 350°C . Calcd (exptl): 22.25% (22.31%). Powder XRD measurement on the calcined

material revealed that $[\text{N}(\text{C}_2\text{H}_5)_4]_2[(\text{UO}_2)_4(\text{OH}_2)_3\text{F}_{10}]$ decomposed to UOF_4 [56].

4. Conclusion

We have successfully synthesized a new uranium oxide fluoride hydrothermally. The new compound has been also characterized by elemental analysis, bond valence calculation, Infrared and Raman spectroscopy, and thermogravimetric analysis. The reported material represents a pseudo-two-dimensional layered structure. Additional experiments using alternate organic templating agents are ongoing and will be reported on them shortly.

5. Supporting information available

Calculated and experimental powder XRD patterns are available (PDF). Crystallographic data (excluding structure factors) for the structure reported in this paper have been deposited with the Cambridge Crystallographic Data Centre as supplementary publication no. CC DC 623686. Copies of the data can be obtained free of charge on application to CCDC, 12 Union Road, Cambridge CB2 1EZ, UK (fax: (44) 1223 336-033; e-mail: deposit@ccdc.cam.ac.uk).

Acknowledgment

We thank the EPSRC for support. We also acknowledge Dr. Christoph Salzmann in obtaining the Raman spectra.

References

- [1] D.W. Breck, Zeolite Molecule Sieves: Structure, Chemistry and Use, Wiley, London, 1974.
- [2] R.M. Barrer, Hydrothermal Chemistry of Zeolites, Academic Press, London, 1982.
- [3] A. Clearfield, Chem. Rev. 88 (1988) 125.
- [4] M.E. Davis, R.F. Lobo, Chem. Mater. 4 (1992) 756.
- [5] P.B. Venuto, Micropor. Mater. 2 (1994) 297.
- [6] P. Feng, X. Bu, G.D. Stucky, Nature 388 (1997) 735.
- [7] A.K. Cheetham, G. Ferey, T. Loiseau, Angew. Chem. Int. Ed. 38 (1999) 3268.
- [8] S. Natarajan, S. Neeraj, A. Choudhury, C.N.R. Rao, Inorg. Chem. 39 (2000) 1426.
- [9] R.A. Laudise, J. Am. Chem. Soc. 81 (1958) 562.
- [10] R.A. Laudise, A.A. Ballman, J. Am. Chem. Soc. 80 (1958) 2655.
- [11] R. Szostak, Molecular Sieves: Principles of Synthesis and Identification, Reinhold, New York, 1989.
- [12] R.J. Francis, M.J. Drewitt, P.S. Halasyamani, C. Ranganathachar, D. O'Hare, W. Clegg, S.J. Teat, Chem. Commun. (1998) 279.
- [13] S.M. Walker, P.S. Halasyamani, S. Allen, D. O'Hare, J. Am. Chem. Soc. 121 (1999) 10513.
- [14] M.B. Doran, S.M. Walker, D. O'Hare, Chem. Commun. (2001) 1988.
- [15] A.J. Norquist, P.M. Thomas, M.B. Doran, D. O'Hare, Chem. Mater. 14 (2002) 5179.
- [16] M.B. Doran, A.J. Norquist, D. O'Hare, Chem. Mater. 15 (2003) 1449.
- [17] J.-Y. Kim, A.J. Norquist, D. O'Hare, Dalton Trans. (2003) 2813.
- [18] A.J. Norquist, M.B. Doran, D. O'Hare, Solid State Sci. 5 (2003) 1149.

Table 4
Infrared and Raman vibrations for $[\text{N}(\text{C}_2\text{H}_5)_4]_2[(\text{UO}_2)_4(\text{OH}_2)_3\text{F}_{10}]$

	IR	Raman
$\delta(\text{U}-\text{F})$		190
		211
$\rho(\text{U}-\text{O})$		235
		255
		274
$\delta(\text{U}-\text{O})$		286
$\nu_{\text{as}}(\text{U}-\text{F})$		347
$\nu_{\text{s}}(\text{U}-\text{F})$	407	414
	432	
	447	
	455	
	458	
	468	
$\nu_{\text{s}}(\text{U}=\text{O})$	850	845
$\nu_{\text{as}}(\text{U}=\text{O})$	857	859
	927	900
$\delta(\text{C}-\text{C}-\text{N})$	472	
$\nu_{\text{as}}(\text{C}-\text{N})$	1053	
$\nu_{\text{as}}(\text{C}-\text{C})$	1070	
$\delta(\text{CH}_2)$	782	1388
	1399	1459
	1455	
$\nu_{\text{s}}(\text{CH}_2)$	2931	2925
$\nu_{\text{as}}(\text{CH}_2)$	2962	2946
$\delta(\text{CH}_3)$	1001	999
	1189	1170
$\nu_{\text{s}}(\text{CH}_3)$	2990	2996
$\nu_{\text{as}}(\text{CH}_3)$	3018	3004
$\delta(\text{OH}_2)$	1654	1666
$\nu(\text{OH}_2)$	3439	3437
	3506	

- [19] A.J. Norquist, M.B. Doran, P.M. Thomas, D. O'Hare, Dalton Trans. (2003) 1168.
- [20] M.B. Doran, C.L. Stuart, A.J. Norquist, D. O'Hare, Chem. Mater. 16 (2004) 565.
- [21] M.B. Doran, B.E. Cockbain, D. O'Hare, Dalton Trans. (2005) 1774.
- [22] A.J. Norquist, M.B. Doran, D. O'Hare, Inorg. Chem. 44 (2005) 3837.
- [23] C.M. Johnson, M.G. Shilton, A.T. Howe, J. Solid State Chem. 37 (1981) 37.
- [24] R. Pozas-Tormo, L. Moreno-Real, M. Martinez-Lara, E. Rodriguez-Castellon, Can. J. Chem. 64 (1986) 35.
- [25] L. Moreno-Real, R. Pozas-Tormo, M. Martinez-Lara, S. Bruque, Mater. Res. Bull. 22 (1987) 19.
- [26] G.J. Hutchings, C.S. Heneghan, I.D. Hudson, S.H. Taylor, Nature 384 (1996) 341.
- [27] D. Grohol, E.L. Blinn, Inorg. Chem. 36 (1997) 3422.
- [28] W.H. Zachariasen, Acta Crystallogr. 7 (1954) 783.
- [29] H. Brusset, N.Q. Dao, A. Rubinstein-Auban, Acta Crystallogr. B 28 (1972) 2617.
- [30] N.Q. Dao, Acta Crystallogr. B 28 (1972) 2011.
- [31] L.K. Templeton, D.H. Templeton, N. Bartlett, K. Seppelt, Inorg. Chem. 15 (1976) 2720.
- [32] P. Joubert, J.M. Weulersse, R. Bougon, B. Gaudreau, Can. J. Chem. 56 (1978) 2546.
- [33] N.W. Alcock, M.M. Roberts, M.C. Chakravorti, Acta Crystallogr. B 36 (1980) 687.
- [34] V.A. Blatov, L.B. Serezhkina, V.N. Serezhkin, V.K. Trunov, Russ. J. Inorg. Chem. 34 (1989) 91.
- [35] P.M. Almond, C.E. Talley, A.C. Bean, S.M. Peper, T.E. Albrecht-Schmitt, J. Solid State Chem. 154 (2000) 635.
- [36] C.E. Talley, A.C. Bean, T.E. Albrecht-Schmitt, Inorg. Chem. 39 (2000) 5174.
- [37] C.L. Cahill, P.C. Burns, Inorg. Chem. 40 (2001) 1347.
- [38] J.-Y. Kim, A.J. Norquist, D. O'Hare, Chem. Mater. 15 (2003) 1970.
- [39] C.-M. Wang, C.-H. Liao, H.-M. Lin, K.-H. Lii, Inorg. Chem. 43 (2004) 8239.
- [40] C.-M. Wang, C.-H. Liao, H.-M. Kao, K.-H. Lii, Inorg. Chem. 44 (2005) 6294.
- [41] P.C. Burns, M.L. Miller, R.C. Ewing, Can. Mineral. 34 (1996) 845.
- [42] P.M. Almond, L. Deakin, M.J. Porter, A. Mar, T.E. Albrecht-Schmitt, Chem. Mater. 12 (2000) 3208.
- [43] S.V. Krivovichev, P.C. Burns, Can. Mineral. 38 (2000) 717.
- [44] S.V. Krivovichev, P.C. Burns, Can. Mineral. 38 (2000) 847.
- [45] R.E. Sykora, D.M. Wells, T.E. Albrecht-Schmitt, Inorg. Chem. 41 (2002) 2697.
- [46] K.M. Ok, M.B. Doran, D. O'Hare, J. Mater. Chem. 16 (2006) 3366.
- [47] P.S. Halasyamani, R.J. Francis, S.M. Walker, D. O'Hare, Inorg. Chem. 38 (1999) 271.
- [48] Z. Otwinowski, Data Collection and Processing, Daresbury Laboratory, Warrington, UK, 1993.
- [49] G. Cascarano, C. Giacobozzo, A. Guagliardi, J. Appl. Crystallogr. 26 (1993) 343.
- [50] L.J. Farrugia, J. Appl. Crystallogr. 32 (1999) 837.
- [51] I.D. Brown, D. Altermatt, Acta Crystallogr. B 41 (1985) 244.
- [52] N.E. Brese, M. O'Keeffe, Acta Crystallogr. B 47 (1991) 192.
- [53] P.C. Burns, R.C. Ewing, F.C. Hawthorne, Can. Mineral. 35 (1997) 1551.
- [54] C.D. Flint, P.A. Tanner, J. Chem. Soc., Faraday Trans. 77 (1981) 2339.
- [55] S.J. Hibble, S.G. Eversfield, A.M. Chippindale, Acta Crystallogr. E 58 (2002) m366.
- [56] J.H. Levy, J.C. Taylor, P.W. Wilson, Inorg. Chem. 14 (1975) 1113.